Transactions, **SMiRT-24**
BEXCO, Busan, Korea - August 20-25, 2017
Division III Paper-03-01-01

NUMERICAL IMPACT SIMULATION FOR PREDICTING RESIDUAL SPEED OF PROJECTILE AFTER PERFORATION

Kazuma Hirosaka[1], Hidekazu Takazawa[1], Katsumasa Miyazaki[2], Norihide Tohyama[3], Satoshi Saigo[4], Hiroyuki Noji[4], and Naomi Matsumoto[4]

[1] Researcher, Center for Technology Innovation-Materials, Hitachi, Ltd., JP
[2] Chief Researcher, Center for Technology Innovation-Materials, Hitachi, Ltd., JP
[3] Chief Engineer, Hitachi-GE Nuclear Energy, Ltd., JP
[4] Engineer, Hitachi-GE Nuclear Energy, Ltd., JP

ABSTRACT

Safety assessments of nuclear power plants should include analyses of aircraft impacting the concrete walls or roofs of the plant buildings. When the outer wall of a building is not thick enough to prevent a projectile from perforating it, the projectile subsequently impacts the inner walls of the structure. Because equipment important for safety is usually housed inside, how far projectiles penetrate inside a structure is an important consideration.

A numerical impact simulation of a projectile perforating a concrete wall was conducted using LS-DYNA®, and the residual speed of the projectile after perforation was compared with test results from other studies. Two kinds of impact simulation were conducted: one of a 100 kg projectile with an impact speed from 150 to 250 m/s (conducted under CRIEPI test conditions; Ito et al. 1991), the other of a 47.4 kg projectile with an impact speed from 80 to 135 m/s (conducted under the international IRIS project impact test conditions; Heckötter and Vepsä 2015). In both simulations, the differences in the residual speeds of the projectiles after perforation from the previous test results were within 10 m/s. As a result, it was concluded that the residual speed after perforation and the energy absorbed by the concrete wall from the impact of the projectile can be evaluated in numerical simulations. Finally, simulations of a commercial aircraft impacting reinforced concrete walls were conducted and the relationship between wall thickness and the residual kinematic energy of the aircraft was revealed.

INTRODUCTION

A safety assessment needs to be conducted to analyze the possible damage caused by aircrafts impacting the concrete walls and roofs of nuclear power plants. Before a nuclear power plant is constructed, it is possible to design the outer concrete wall to be thick enough to prevent an impacting aircraft from perforating it. In that case, we only need to evaluate whether the outer wall is perforated or not; after confirming that the outer wall will not be perforated, designers can be assured that the area damaged by the impact is limited to the outer wall. On the other hand, aircraft impact analyses of existing nuclear power plants must assume that the aircraft perforates the outer wall of a concrete structure and crashes into its inner structures, because the outer wall has already been constructed and its thickness cannot easily be changed into one thick enough to prevent an aircraft from perforating it. In this case, sequential impacts on the walls inside the outer wall need to be considered in order to predict how far an aircraft will go inside the structure and the area physically damaged by the impact. The Nuclear Energy Institute in the U.S. published NEI 07-13, a guideline of a methodology for aircraft impact analysis to evaluate the stability of nuclear power plants (Nuclear Energy Institute 2011), and the guideline also describes the method of evaluating sequential impacts on concrete walls by aircraft.

The local destruction modes of concrete due to the impact of a projectile are classified into penetration, scabbing, and perforation, and empirical equations for predicting the destruction mode of a concrete wall have been established on the basis of many impact tests. The modified NDRC equation (National Defence

Research Committee 1946), Chang equation (Chang 1981), and Degen equation (Degen 1980) are representative empirical equations that predict the penetration depth of a concrete wall, the concrete thickness at which scabbing starts to occur, and the concrete thickness at which perforation starts to occur. We can estimate the distance a projectile will reach and evaluate the physically damaged area when a projectile perforates a reinforced concrete (RC) wall and crashes into the inner wall if the residual speed of the projectile after perforation can be predicted. Kar (Kar 1979) described a method for estimating the projectile speed after perforation that can be used when a concrete wall is locally perforated by a projectile. CRIEPI conducted an impact test in which the residual speeds of projectiles were measured after they had perforated a concrete wall. The international project named IRIS conducted similar impact tests with rigid projectiles and measured the projectile speed after perforation.

In this study, we conducted numerical simulations of impacts on concrete walls. We selected the dynamic finite element program LS-DYNA®, because many impact simulations of RC targets have used this program (Agardh 1999, Tai 2006) and it has been recognized as one of the best codes for simulating impact phenomena. First, we checked whether the impact simulation with solid projectile was applicable for the prediction of its residual speed after perforation of RC wall. For this purpose, simulated projectile speeds after perforation of the wall were compared with test results from the CRIEPI and IRIS projects, and the comparison validated the concrete model used in the impact simulation. We also compared the simulation results with estimations made using the Kar method and found that this method is reasonably good at estimating the projectile speed after perforation. Second, we tried to understand the outline of the physical damage in existing power plants by aircraft impact. For this purpose, we conducted a simulation of a commercial aircraft impacting an RC wall and obtained a relationship describing the reduction in the kinetic energy of the aircraft caused by perforation. Using these simulation results, we can predict how far the aircraft goes inside a building after sequential impacts into RC walls.

IMPACT SIMULATION OF RIGID PROJECTILE

Impact Simulation of CRIEPI Impact Test

CRIEPI conducted several impact tests in the 1990s. In these tests, rigid projectiles impacted an RC wall that was supported by a back-up structure. Table 1 shows some of the test conditions. The mass of the projectile was 100 kg, and the wall thickness was 400 mm. We conducted our impact simulation under these test conditions and compared the simulation results with the test results.

Figure 1 shows a schematic outline of the RC wall (a quarter of the wall). The wall measured 2500 mm × 2500 mm × 400 mm. Reinforced bars (rebar) were buried 25 mm beneath the front surface laterally and longitudinally as shown in Figure 1, and same amount of rebar was buried 25 mm beneath the back surface as well. The interval of rebar was 100 mm all over.

Figure 2 shows the simulation model of the RC wall. The concrete model called KCC (Karagozian & Case Concrete; Crawford et al. 2011) was used for simulating the concrete material. The concrete elements consisted of solid elements that turned into SPH (Smoothed Particle Hydrodynamics) elements when the minimum principal strain of the solid element reached a certain criterion. In this study, we referred to a study of concrete behaviour at impact (Kennedy 1976) and used the value of -0.0065 for the criterion. The mesh size of the solid elements was a 50 mm cube, and one solid element turned into one SPH element. Each rebar was modelled using 50-mm beam elements and the connection of the rebar inside concrete was modelled by sharing the beam nodes with the solid nodes. Because the element size of the concrete solid was 50 mm, the distance of each rebar from the front concrete surface in simulation model was 50 mm and 0 mm from the back surface. Support plates for the RC wall were set at corners of the RC wall in the test equipment, and these supports were modelled with solid elements in the simulation and their back sides were fixed boundary conditions. Figure 2 shows the shape of the supports that consisted of two plates (350 mm × 350 mm × 25 mm) and one bar (50 mm × 50 mm × 350 mm) between them. The rigid projectile was modelled by solid elements, and its radius and weight were same as those of the projectile used in the test.

Table 2 shows the material properties of the simulation model. We used properties described in the test report and typical properties for ones which were not described in the report. We used a fracture strain of 0.06 for the rebar in order to consider the possibility of the bars fracturing at the moment of perforation. This value was determined from the fracture strain of rebar of 0.05 denoted in NEI 07-13.

Table 1 Conditions of impact test conducted by CRIEPI (Ito et al. 1991)

Projectile			RC wall		
Diameter [m]	Mass [kg]	Impact speed [m/s]	Thickness [m]	Rebar ratio % (one side)	Compressive strength [MPa]
0.23	100	150, 200, 250	0.4	0.5	23.5

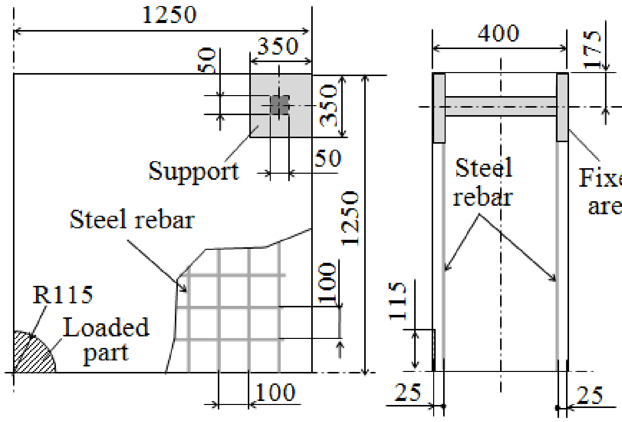

Figure 1 RC wall in impact test (upper right quarter) (Unit: mm)

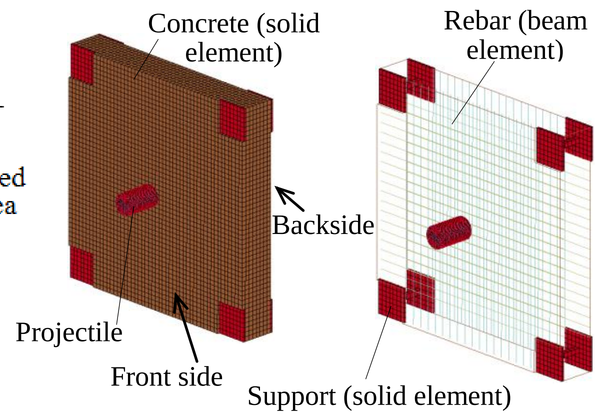

Figure 2 Simulation model of RC wall

Table 2 Material properties for simulation model

	Reinforced Concrete (RC)	Steel rebar, Support
Density [kg/m^3]	2500	7850
Poisson ratio [-]	0.19	0.3
Young's modulus [GPa]	23	205.9
Compressive strength [MPa]	23.5	490

Figure 3 shows the relationship between the initial speed of the projectile and its speed after perforation (Solid circle denotes the test results, open triangle the simulation results, the solid line the estimation using Kar's method). Kar's method for estimating the residual speed of the projectile after perforation is as follows:

(1) Calculate the initial speed of the projectile at which the projectile just perforates the RC wall used in the test. Here, "just perforates" means that the residual speed of the projectile after perforation is 0 m/s. The Degen equation (Degen 1980) is used for this calculation.

(2) Calculate the residual speed of the projectile after perforation (V_r) by using equation (1) together with the obtained speed of a "just perforation" (V_p) and the initial impact speed of the projectile (V_i); the equation is derived from the conservation of kinetic energy before and after the impact of projectile:

$$\frac{1}{2}mV_i^2 = \frac{1}{2}mV_p^2 + \frac{1}{2}(m+M)V_r^2 \quad . \tag{1}$$

Here, m is projectile mass, and M is mass of the fractured pieces of concrete at impact, as estimated by equations (2):

$$\begin{cases} M = \pi \cdot \rho_c \cdot \dfrac{h}{3} \cdot (R^2 + R \cdot R_2 + R_2^2) \\ R_2 = R + h \cdot \tan\theta, \quad \theta = \dfrac{45°}{(h/2R)^{\frac{1}{3}}} \le 60° \end{cases} \quad . \tag{2}$$

Here, ρ_c is concrete density of the RC wall, h is thickness of the RC wall, and R is radius of the projectile. Equations (2) are derived from the relation between the sizes of the projectile and wall.

Figure 3 shows that the simulation results are in good agreement with the test results; the differences between the simulation and test results are within 10 m/s. Moreover, the results of Kar's method are almost the same as the test results.

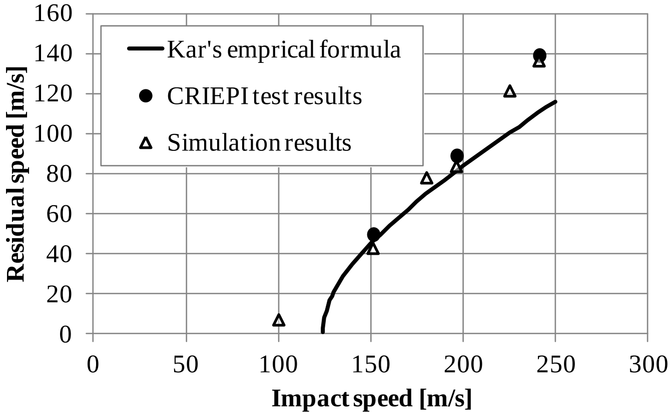

Figure 3 Comparison of residual speeds of projectile after perforation in CRIEPI impact test

Impact Simulation of Impact Test in IRIS Project

The international research project titled "Improving Robustness Assessment Methodologies for Structures Impacted by Missiles (IRIS)" conducted several impact tests in which rigid projectiles impacted RC walls (OECD-NEA, 2014). The speed of the projectile after it perforated the RC wall was measured in a number of cases. We compared the results of an impact simulation conducted under the same conditions as IRIS with the test results of IRIS.

Table 3 shows the test conditions. Each test result includes the speed of the projectile after perforation. Figure 4 shows photographs of the test facility. The projectiles impacted an RC wall that was fixed to a support frame. Figure 5 shows the outline of the concrete wall. The wall measured 2100 mm × 2100 mm × 250 mm. A grid of 24 reinforced bars (rebar) was buried beneath the front surface and another such grid was buried beneath the back surface.

Table 3 Outline of impact tests (Heckötter and Vepsä 2015)

Component	Specifications
Projectile	Steel pipe filled with light concrete: 47.5 kg, Diameter: 168.3 mm Impact speed: 136 m/s, 120 m/s, 110 m/s, 102 m/s, 100 m/s
Concrete	Height: 2100 mm, Width: 2100 mm, Thickness: 250 mm
Rebar	Number: 24 × 24 (lateral and longitudinal), Interval: 90 mm, Diameter: 10 mm

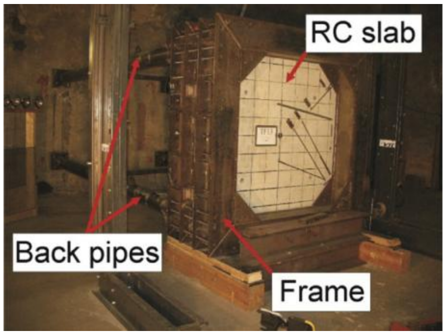

(a) Overview of test facility

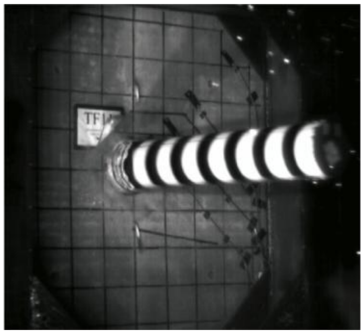

(b) Photograph of impact moment

Figure 4 Photographs of the test facility (Heckötter and Vepsä 2015)

Figure 6 shows the simulation model of the RC wall. The interval of the rebars in the test was 90 mm; thus, the concrete solid elements in the simulation were set to be 45 mm × 45 mm × 50 mm, and the rebar beam elements were set to be 45 mm. The connections of the rebar inside a concrete were modelled by sharing the nodes of the beam elements with the solid elements. The thickness of the concrete element was 50 mm; the distance of the rebars from the concrete surface in the simulation model was set to be 50 mm, whereas the distance of the rebars from the concrete surface in the test wall was about 40 mm

The picture of the test wall shows that it was fixed to a surrounding support: thus, the RC wall in the simulation was fixed in the same way. A support plate was set at each corner of the concrete wall and was modeled by solid elements in the simulation. Figure 6 shows the shape of the support; it consisted of two plates (225 mm × 225 mm × 50 mm) and one bar (45 mm × 45 mm × 150 mm) between them. The red elements in Figure 6 show the whole support elements including the support plate and support elements surrounding the RC wall. The support elements were made of iron material and we used the typical properties for these elements. We fixed the back side of all the support elements as a boundary condition.

Table 4 shows the specifications of the concrete used in the simulation; the concrete strength was 70 MPa. Accordingly, the parameters of the concrete model were modified on the bases of these specifications. Table 4 also shows the specifications of the rebar simulation model; these data were determined from the document. The fracture strain of the rebar was set to 0.06 (as in section 3.1), and the concrete elements were solid elements that turned into SPH elements when the minimum principal strain of the solid element reached 0.0065, the same as in section 3.1.

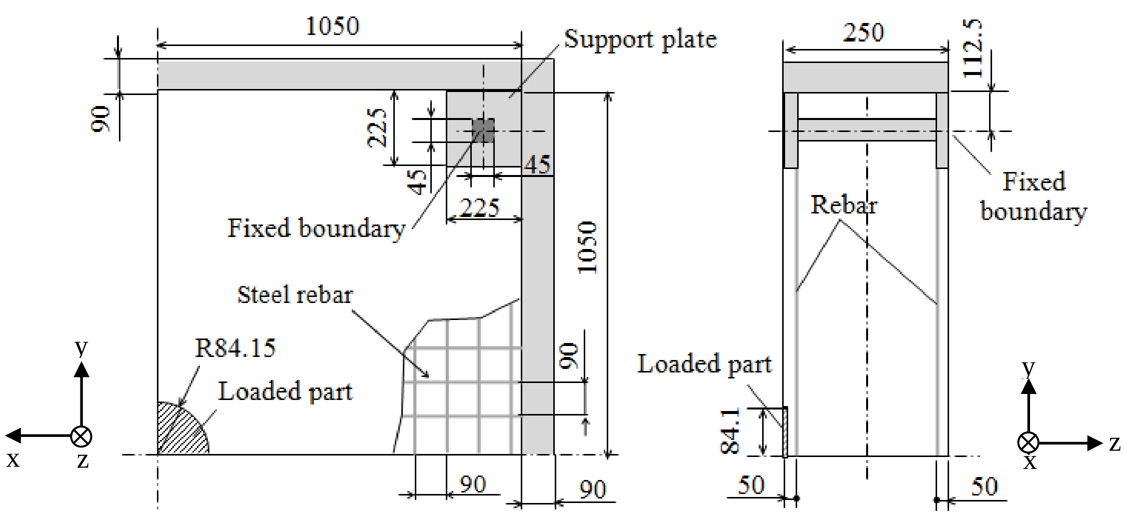

Figure 5 Size and boundary conditions of upper right quarter of wall (Unit: mm)

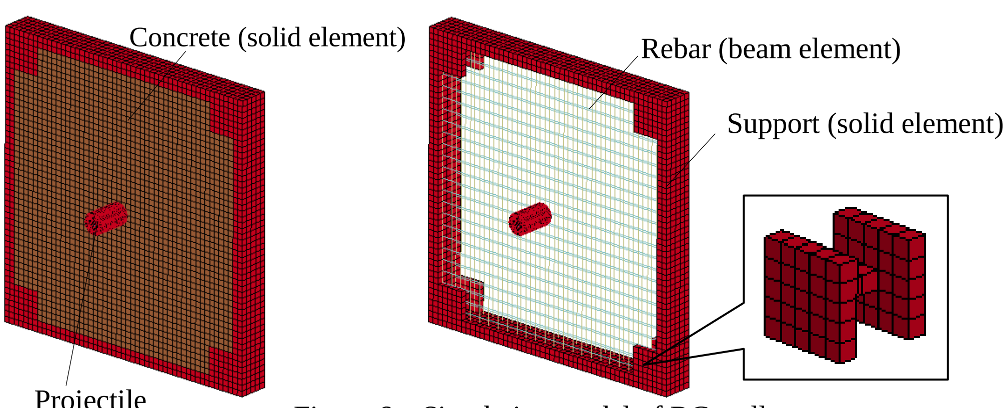

Figure 6 Simulation model of RC wall

Table 4 Material properties for simulation model

	Reinforced concrete (RC)	Steel rebar, Support
Density [kg/m^3]	2500	7850
Poisson ratio [-]	0.19	0.3
Young's modulus [GPa]	37	210
Compressive strength [MPa]	70	420

Figure 7(a) shows the state of the RC wall in the simulation after the impact of a projectile at 140 m/s. The destruction mode is perforation. Figure 7(b) shows the state of the concrete wall in test after the impact of a projectile at 136 m/s. The destruction mode is perforation, and the mode is the same as in the simulation results. The destruction modes at different impact speeds (120 m/s, 110 m/s, 100 m/s, 80 m/s) were all perforation in the simulation, and test results for impact speeds over 100 m/s were also perforation. Thus, the simulation results reproduced the test results.

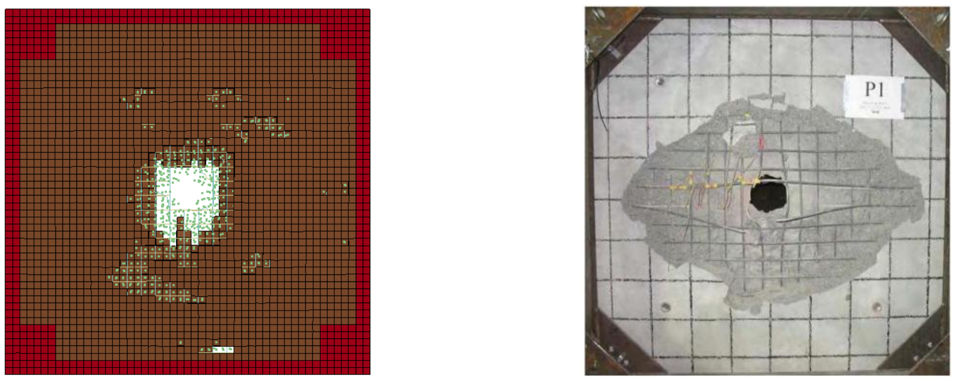

(a) Simulation (Speed: 140 m/s) (b) Test (Speed: 136 m/s) (Heckötter and Vepsä 2015)

Figure 7 Comparison of destructed states of simulated and actual RC walls at impact

Figure 8 shows the relationship between the initial speed of an projectile and its speed after perforation (Solid triangle indicates test results, and open circle the results of simulations conducted by the Technical Research Centre of Finland (VTT) (Heckötter and Vepsä 2015), red open circle indicates the simulation results of this study, and the solid line estimates from Kar's method. The procedure of Kar's method is described in section 3.1).

The figure shows that the simulation results are in good agreement with test results and the difference between simulation and test results are within 10 m/s. The estimates given by Kar's method are almost the same as the test results. The simulation results in this study are almost the same as the simulation results by VTT, and both simulation results reproduce the test results with similar preciseness.

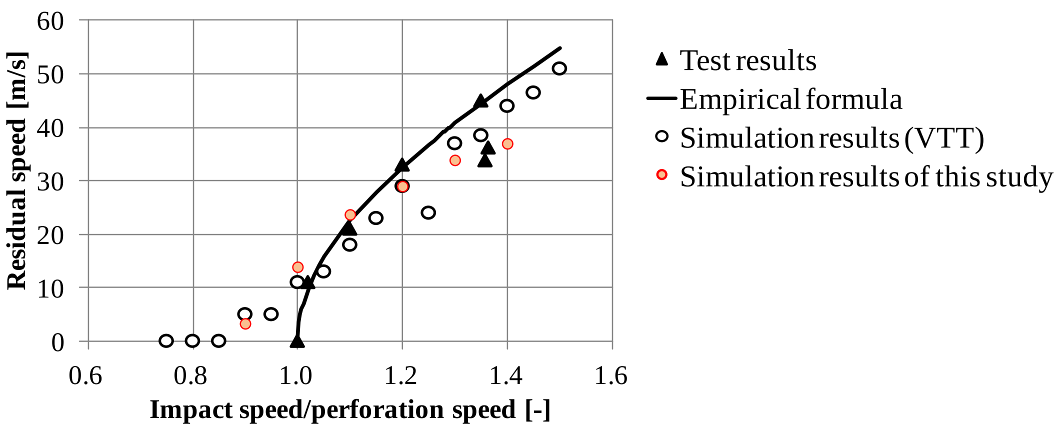

Figure 8 Residual speeds of projectile after perforation in IRIS impact test

DISCUSSION OF IMPACT SIMULATION OF COMMERCIAL AIRCRAFT

One of the methods to estimate how far the aircraft goes inside a building is counting how many walls are perforated before the aircraft stops. For this, we need to predict the aircraft speed after it perforates the reinforced concrete (RC); that is, we need to predict reduction in aircraft kinematic energy when the aircraft perforates. We can use the results of a simulations that investigate the kinematic energy reduction because of perforation of several concrete of varying thickness and strength for predicting the area affected by the aircraft impact. The relationship between the concrete thickness and the aircraft kinematic energy reduction depends on an aircraft type, impact speed and impact direction; thus, when the analyses with large type aircraft impacting at the vertical angle to RC wall at high speed are considered, the simulation results using these conditions can be used as the worst-case scenario. There is no need to conduct simulations of cases other than the worst-case scenario; hence, simulating only the worst-case scenario reduces the overall simulation cost.

Table 5 shows the specifications of the reinforced concrete (RC) wall. The impact simulations were used to obtain the aircraft speeds and mass after the wall was perforated. Using these results, we estimated the relationship between wall thickness and aircraft kinematic energy reduction.

Table 5 Specifications of concrete wall

No.	Thickness (mm)	Diameter of rebar (mm)	Interval of rebar (mm)	Number of rebar layers	Compressive strength of concrete (MPa)
1	250	D13	200	1 on each side	33
2	450	D16			
3	600	D19			
4	800	D29			
5	1000	D35			

Figure 9 shows the simulation models of the aircraft and RC wall. Shell elements and SPH elements were used for the aircraft model. The fuselage, wing, and nacelle consisted of shell elements. The fuel, engine equipment, and weight on board, such as system equipment, undercarriage, and payload, consisted of SPH elements. The shell elements were given the material properties of aluminium alloy utilized in aircraft. The RC wall was modelled in the same way as described in the previous section, and hybrid elements, which were solid elements that turned into SPH elements given some criteria, were used. In Figure 9, the shell elements of the aircraft are grey, the SPH elements of fuel are blue, the the SPH elements of the engine equipment inside the nacelle and weight on board contained inside the fuselage are purple, and the SPH elements of the concrete wall are green. Figure 10 shows the dimensions of the RC wall and boundary conditions. The height was 9 m, about a height of a single-story concrete structure, and the width was 60 m. The smaller the interval between each column inside wall is, the larger the resistance of the RC wall against an aircraft impact becomes; hence, we did not distribute any columns inside the wall within a width of 60 m and conservatively predicted the aircraft speed after it perforated the RC wall. The solid line of the outer wall indicates that a floor and a ceiling of a building exist behind the wall, and the boundary conditions on these 2 faces of the outer wall fixed the displacement in z direction. The dotted line of the outer wall indicates that side walls of a building exist behind the wall and the boundary conditions on these 2 faces fixed the transitional displacement. Grids of reinforced bars (rebar) were installed on both sides of the wall.

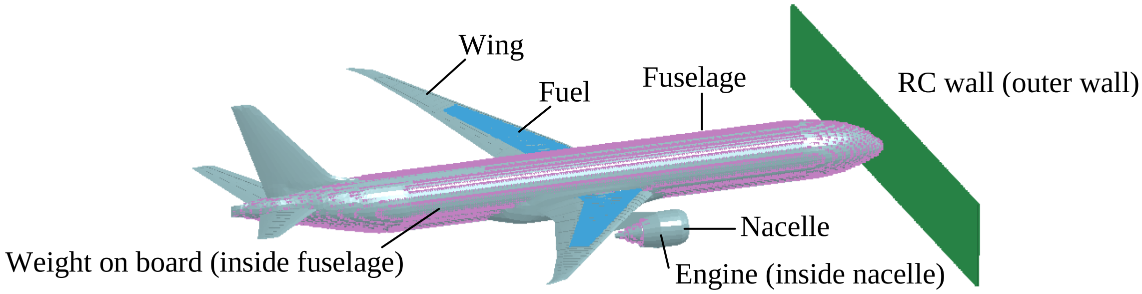

Figure 9 Simulation model for predicting speed reduction by perforation

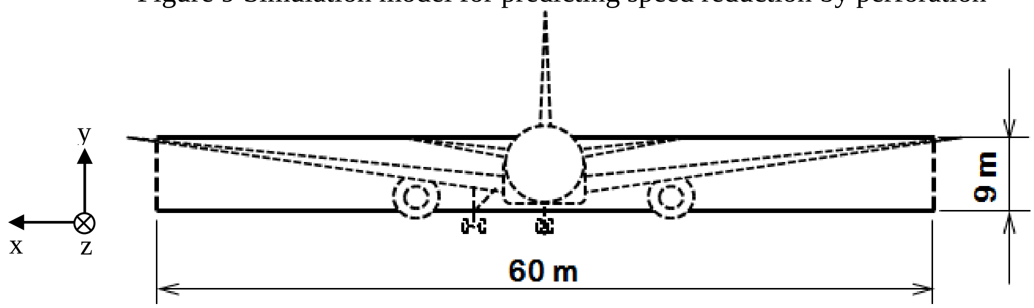

Figure 10 Size of RC wall model for impact simulation of commercial aircraft

Figure 11 shows the simulation results for case No. 1 in Table 5. It shows that the fuel, payload, and systems such as electrical system and flight control system contained inside the fuselage and pieces of concrete dispersed after impact. Figure 11(a) shows only the shell elements in the simulation; the wings and engines went inside the wall, but they dropped off at impact even though the thickness of the concrete wall was only 250 mm. Figure 12 shows the results for case No. 5 in Table 5; in this case, the engine dropped off outside the thick outer wall (1000 mm thick). These results indicate that the fuselage penetrates further inside the building than the wings or engines.

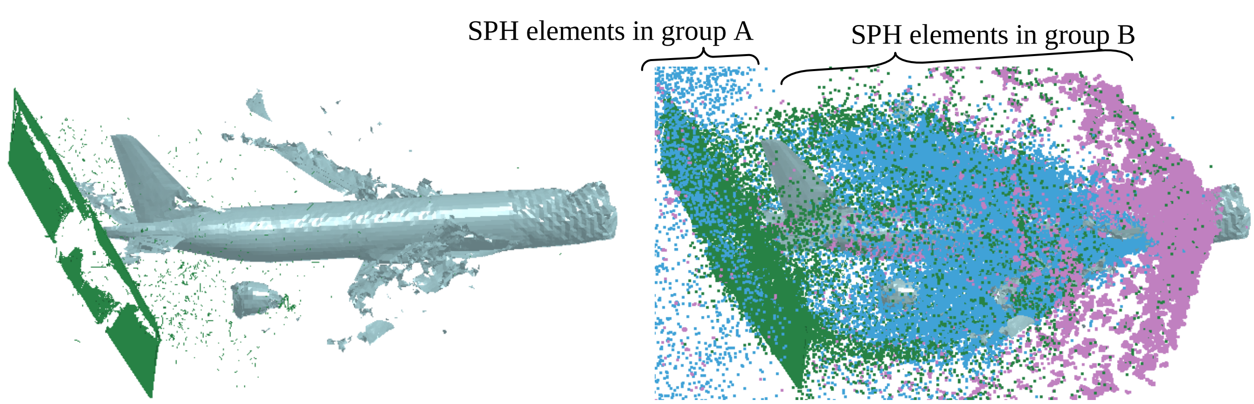

(a) After impact (SPH elements are hidden) (b) After impact (SPH elements are displayed)

Figure 11 Impact simulation with 250-mm-thick RC wall

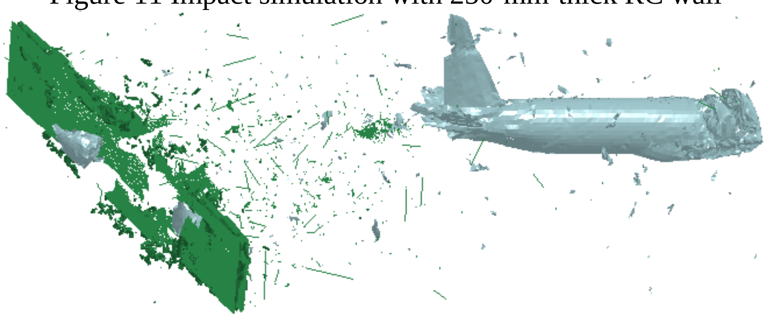
Figure 12 Impact simulation with 1000-mm-thick RC wall (SPH elements are hidden)

We can predict how far the aircraft goes inside the building if reduction in kinematic energy due to the impact with the RC wall is known because the aircraft stops at the moment when the kinematic energy of the aircraft becomes 0 J during the sequential impact with the RC walls.

The reduction in kinematic energy of the aircraft is as follows:

$$\text{Reduction in kinetic energy of aircraft} = \frac{1}{2}M_0V_0^2 - \frac{1}{2}MV^2 \quad (3)$$

Here, M_0 is mass of the aircraft, V_0 is impact speed, M is mass of the aircraft after perforation, and V is the speed after perforation. If the engines and main wings drop off, M does not include these masses. M and V are obtained from the simulation results, and V is the speed measured at the end of the fuselage. M is the sum of the masses of the shell elements and SPH elements. Some SPH elements bounce back at the moment of impact, as shown in Figure 12(b), where the SPH elements in group A bounce back, but the SPH elements in group B go inside the RC wall. The SPH elements in group B potentially affect the inner walls; therefore, when we calculated M from the simulation results, we counted the whole mass of the SPH elements in group B, which do not bounce back at impact.

Figure 13 shows the relationship between the reduction in aircraft kinetic energy and RC wall thickness. As the wall thickness increases, the reduction in aircraft kinetic energy at impact increases. The effect of the engine and main wings dropping off are indicated by the red background in the figure; they have the most effect on the reduction in the kinetic energy.

The engines and main wings drop off in the first of the sequential wall impacts; they do not fall off when the fuselage impacts the inner walls inside the building. Thus, the amount of kinetic energy in the red background should not be counted when the reduction in kinetic energy is estimated using Figure 13 for impacts on the inner walls.

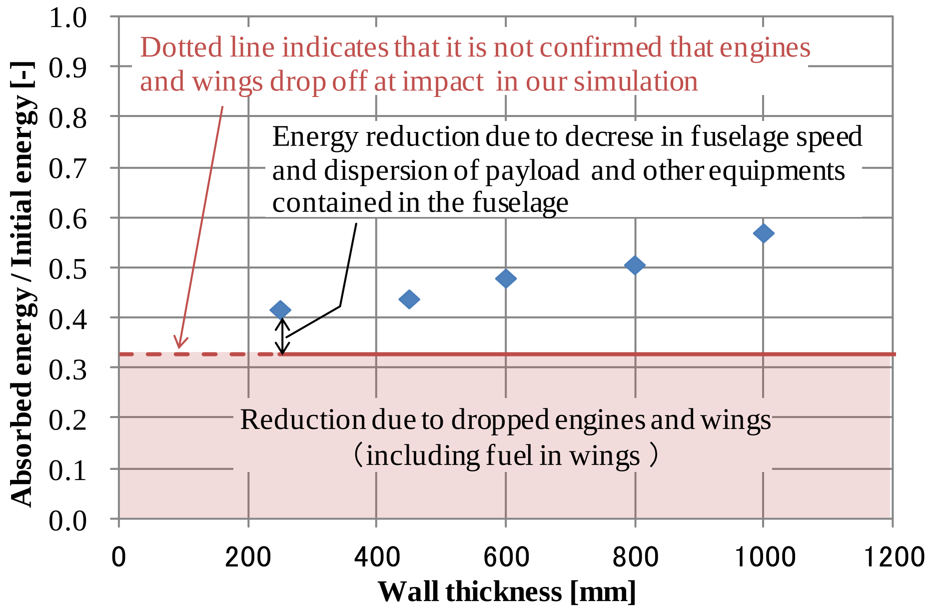

Figure 13 Relationship between wall thickness and reduction in kinetic energy

CONCLUSION

We conducted impact simulations of rigid projectiles and commercial aircraft crashing into the RC walls. Our findings are summarized as follows:

・ In the simulations representing the impacts of rigid projectiles, the destruction mode of the RC wall and the residual speed of a projectile after perforation were compared with the test results, and it was found that the simulation results are in a good agreement with the test results.

・ In the impact simulation of a commercial aircraft crashing into an RC wall, the reduction in aircraft kinetic energy caused by the perforation of the RC wall was estimated. By referring to these simulation results, we can predict how far the aircraft goes inside the building. It is also found that the engines and main wings drop off at impact even if the thickness of the RC wall is only around 250 mm.

・ The aircraft impact simulations using the RC wall which consists of solid elements that turned into SPH elements and the aircraft model which consists of shell and SPH elements are useful for aircraft impact analysis.

REFERENCES

Agardh, L. and Laine, L. (1999). "3D FE-simulation of high-velocity fragment perforation of reinforced concrete slabs", *International Journal Impact Engineering*, 22, 911-922.

Chang, W. S. (1981). "Impact of solid missiles on concrete barriers," *Journal of the Structural Division ASCE*, 107, ST2, 257-271.

Crawford, J. E., Wu, Y., Choi, H., Magallanes, J. M., and Lan, S. (2011). "Use and Validation of the Release III K & C Concrete Material Model in LS-DYNA," *TR-11 36-5*, Karagozian & Case, USA

Degen, P. O. (1980). "Perforation of reinforced concrete slabs by rigid missiles", *Journal of the Structural Division ASCE*, 106, ST7, 1623-1642.

Ito, C., Onuma, H., Shirai, K. (1991). "Design Method of Concrete Structures against Impact due to Collision of Missile", *CRIEPI Research Report*, U24.

Kar, A. K. (1979). "Residual Velocity for Projectiles", *Nuclear Engineering and Design*, 53

Kennedy, R. P. (1976). "A review of procedures for the analysis and design of concrete structures to resist missile impact effects", *Nuclear Engineering and Design*, 37, 183-203

National Defence Research Committee. (1946). "Effects of impact and explosion," *Summary Technical Report of Division 2*, 1, USA.

Nuclear Energy Institute. (2011). "Methodology for Performing Aircraft Impact Assessments for New Plant Designs," *NEI 07-13 Revision 8*, USA

Tai, Y. and Tang, C. (2006). "Numerical simulation: The dynamic behaviour of reinforced concrete plates under normal impact", *Theoretical and Applied Fracture Mechanics*, 45, 117-127.

Heckötter, C., and Vepsä, A. (2015) "Experimental investigation and numerical analyses of reinforced concrete structures subjected to external missile impact", *Progress in Nuclear Energy*, 84, 56-67

Organisation for Economic Cooperation and Development Nuclear Energy Agency (OECD-NEA). (2014) "Improving Robustness Assessment Methodologies for Structures Impacted by Missiles (IRIS-2012) final report"